ACS APPLIED MATERIALS & INTERFACES

Research Article

www.acsami.org

Near-Infrared-Triggered Anticancer Drug Release from Upconverting Nanoparticles

Laura L. Fedoryshin, Anthony J. Tavares, Eleonora Petryayeva,† Samer Doughan, and Ulrich J. Krull*

Chemical Sensors Group, Department of Chemical and Physical Sciences, University of Toronto Mississauga, 3359 Mississauga Road, Mississauga, Ontario L5L 1C6, Canada

Supporting Information

ABSTRACT: Targeted drug delivery using functional nanoparticles has provided new strategies for improving therapeutic efficacy while concurrently minimizing toxicity. Photodynamic therapy is an approach that offers control of drug delivery by use of an external photon source to allow active therapeutic release to a target area. Upconverting nanoparticles (UCNPs) have potential to operate as integral components of photodynamic therapeutic platforms based on the resonant absorption of near-infrared (NIR) radiation and emission at shorter wavelengths. NIR radiation is minimally absorbed and scattered by biological tissues, and the NIR excitation of UCNPs can generate anti-Stokes emission in the ultraviolet−visible wavelength range at intensities that can be used to trigger cleavage of bonds linking therapeutics at the nanoparticle interface. Herein, we describe an investigation of photocleavage at the surface of UCNPs to release the chemotherapeutic 5-fluorouracil (5-FU). Core−shell UCNPs composed of a β-$NaYF_4$: 4.95% Yb, 0.08% Tm core and a β-$NaYF_4$ shell were coated with *o*-phosphorylethanolamine ligands and coupled to an *o*-nitrobenzyl (ONB) derivative of 5-FU. NIR excitation of the UCNPs resulted in photoluminescence (PL) emission bands centered at 365, 455, and 485 nm. The UV−blue PL was in resonance with the absorption band of the ONB−FU derivative resulting in photocleavage and subsequent release of the 5-FU drug from the UCNPs for these *in vitro* studies. The release of 5-FU was complete in <14 min using a NIR laser source centered at 980 nm that operated at a power of <100 mW. The efficiency of triggered release was as high as 77% of the total ONB−FU conjugate, while the rate of drug release could be tuned with the laser power output. This work provides an important first step in the development of a UCNP platform capable of targeted chemotherapy.

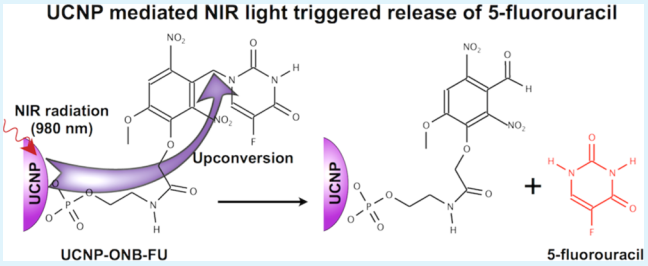

KEYWORDS: *lanthanide, upconverting nanoparticles, photolysis, drug delivery, near-infrared, 5-fluorouracil*

INTRODUCTION

The targeted delivery of therapeutic agents *in vivo* using functional nanoparticles (NPs) has attracted attention as a method for minimizing the side effects and toxicity of chemotherapy.[1−3] The use of NPs has been facilitated by the ability to concurrently link both tumor targeting groups and pharmaceutical compounds to the surface of a NP. Numerous delivery mechanisms, varying from micellar and polymeric encapsulation to active cleavage of drugs from NP surfaces using cellular enzymes, have been proposed for the selective delivery of compounds to diseased tissues.[4] An alternate approach is photodynamic therapy (PDT), which involves the use of light to trigger therapeutic delivery. Typically photodynamic therapy makes use of ultraviolet−visible (UV−vis) excitation, often to produce a reactive oxygen species (ROS) by induction of chemical reactions of photosensitive agents.[5,6] This approach is effective but can be limited in practical application by the poor tissue penetration of UV−vis radiation, the limited library of photosensitizing agents that are available, and the hydrophobic nature of many of these compounds. The use of near-infrared (NIR) radiation within the spectral range of 600−1300 nm for PDT allows for greater depth of penetration of radiation into tissues as absorbance and scattering by skin, blood, water, and lipids is minimal.[7] However, the energy associated with NIR radiation is insufficient to provide the electronic excitation that is required to activate PDT agents.

Upconverting NPs (UCNPs) offer potential for the development of platforms from which to build PDT delivery systems that can release therapeutic agents to a specific site. Upconversion is a process that converts NIR radiation into higher-energy UV−vis radiation, as would be required for the activation and release of a toxic reagent. Core−shell UCNPs composed of $NaYF_4$ nanocrystals (host matrix) doped with lanthanides such as Tm^{3+} (activator) and Yb^{3+} (sensitizer) can convert continuous 980 nm laser radiation into a few narrow higher-energy emission bands in the UV−vis range. The upconversion luminescence originates from intraconfigurational 4f transitions of lanthanide dopants. By variation of the dopant concentration, the emission spectra can be tuned.[8] During upconversion, two or more photons are absorbed and

Received: May 19, 2014
Accepted: August 4, 2014
Published: August 4, 2014

   dx.doi.org/10.1021/am503039f | ACS Appl. Mater. Interfaces 2014, 6, 13600−13606

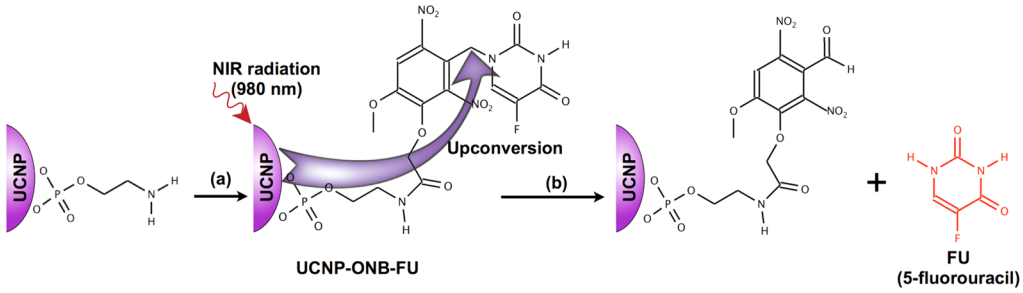

Figure 1. (a) Modification of water-soluble β-$NaYF_4$: 4.95% Yb, 0.08% Tm/β-$NaYF_4$-doped core−shell *o*-phosphorylethanolamine-capped UCNPs with ONB-FU. (b) NIR excitation (980 nm) of the UCNPs resulted in upconverted PL emission at 364 nm used for photocleavage of the ONB−FU bond and subsequent release of 5-fluorouracil from the UCNP surface. Drawing is not to scale.

combined through excited state absorption, energy transfer, or photon avalanche mechanisms.[8] Upconversion takes place with two or more photon absorptions occurring in sequence rather than simultaneously, eliminating the need for high-power density pulsed lasers like those used in two-photon excitation. UCNPs are also advantageous because of the biocompatibility of the material composition and their usefulness in optical diagnostic applications because of their high photostability, weak background signal, and long luminescence lifetimes (micro- to milliseconds).[9]

The advantages of UCNP-mediated PDT have been confirmed.[10] The adsorption of a therapeutic to the NP surface,[11−13] the use of a mesoporous shell or micelle for drug release,[14−16] the activation of photosensitizing agents,[17−20] the delivery of active enzymes,[21] and payload-carrying polymer depolarization[22] have been reported. The former two approaches are compromised by inherent instability associated with physical adsorption or encapsulation of therapeutic agents that result in loss over time, while the latter has shown improved control compared to that with on-demand delivery or localized therapy. Active PDT was reported in a study by Cui et al. that utilized UCNPs decorated with the photosensitizer zinc(II) phthalocyanine.[19] Upconversion photoluminescence (PL) bands at 540 and 660 nm were used for *in vivo* tumor imaging and generation of ROS through the transfer of energy to the interfacial zinc photosensitizer, respectively. Folic acid (FA) was co-immobilized for targeted therapy. UCNP-triggered ROS generation displayed 50% tumor inhibition compared to the 18% when visible light was used as the excitation source.[19]

UCNPs tagged with FA and doxorubicin (DOX) were used in a study by Chien et al. for targeted chemotherapy.[23] FA ligands were caged using the photolabile nitrobenzyl (NBz) group through covalent attachment to the carbohydrate moiety of the FA molecule. Laser excitation at 980 nm was used to produce UCNP PL at 360 nm, and this short wavelength resulted in uncaging of FA by excitation of the NBz group. The system was used for targeted tumor binding to cell surface FA receptors. DOX was coupled to the UCNP surface via a labile disulfide bond and released intracellularly through cleavage by lyosomal enzymes after internalization of NPs, and inhibition of tumor growth was noted.[23] Photoactivation of platinum prodrugs has also been reported using the upconverted PL emission from UCNPs. UV PL from UCNPs was utilized to activate the dicarboxyl *trans*-platinum(IV) prodrug to the highly toxic Pt(II) derivative to kill cancerous cells, with efficacy tracked *in vivo* using trimodal imaging with PL, computer tomography, and magnetic resonance.[17]

In the work reported here, we describe UCNP-mediated drug release that utilizes the *o*-nitrobenzyl (ONB) photolabile tether reported by the Rotello group[24] to allow caging of the well-known chemotherapeutic 5-fluorouracil (5-FU). The ONB group is a popular photolabile protecting group and was originally introduced by Patchornick, Amit, and Woodward.[25] The ONB group undergoes photolytic cleavage upon irradiation at 365 nm, allowing for the controlled release of the covalently attached therapeutic. Core−shell UCNPs composed of β-$NaYF_4$: 4.95% Yb, 0.08% Tm were made water-soluble by being coated with *o*-phosphorylethanolamine. The primary amine functional group from the ligand was coupled to the carboxylic group of the ONB−FU molecule (Figure 1). Upon excitation with NIR radiation at 980 nm, anti-Stokes-shifted UV PL from the UCNPs caused photocleavage of the ONB group. The release of 5-FU was quantitatively monitored using high-performance liquid chromatography (HPLC). Given the greater tissue penetration depth of NIR radiation compared to UV wavelengths, UCNP-mediated drug release has the potential to offer an attractive approach for targeted delivery *in vivo*. The main advantage of this approach is two-fold. The ONB linker provides a robust, stable, and facile coupling method for self-assembly of the 5-FU on the surface of the UCNPs. In addition, the kinetics of photocleavage are on the order of minutes, and the release rate is proportional to the power of the incident photon source. Reports in the literature have utilized a photolabile NBz group for uncaging of FA targeting ligands for tumor imaging applications to allow site specific labeling.[23] In this approach, the ONB linkage offers excellent control over the amount of therapeutic released. Moreover, the ONB group can be covalently attached to a variety of therapeutics, and this strategy could find application to a broad range of photosensitizing agents and chemotherapeutic drugs. This preliminary *in vitro* work is an important first step in the development of surface chemistry that is suitable for designing UCNPs that ultimatley may be used for *in vivo* imaging and effective delivery of chemotherapeutics.

EXPERIMENTAL SECTION

Synthesis of Core−Shell Oleic Acid-Capped β-$NaYF_4$: Yb, Tm UCNPs. For the synthesis of the cores, a typical procedure involved adding 0.4586 g of $Y(CH_3CO_2)_3$, 0.2527 g of $Yb(CH_3CO_2)_3$, and 0.0042 g of $Tm(CH_3CO_2)_3$ to a 150 mL three-neck round-bottom flask along with 30 mL of 1-octadecene and 12 mL of oleic acid while the mixture was being stirred. The reaction mixture was heated to 115 °C for 30 min under vacuum. The temperature was then decreased to 50 °C under an argon atmosphere. Subsequently, 20 mL of a methanol solution with 0.2966 g of NH_4F and 0.1904 g of NaOH was added to the reaction mixture, and it was allowed to stir for an additional 30 min. The cloudy solution was heated to 70 °C to remove excess methanol. The temperature was then increased to 300 °C and

dx.doi.org/10.1021/am503039f | ACS Appl. Mater. Interfaces 2014, 6, 13600−13606

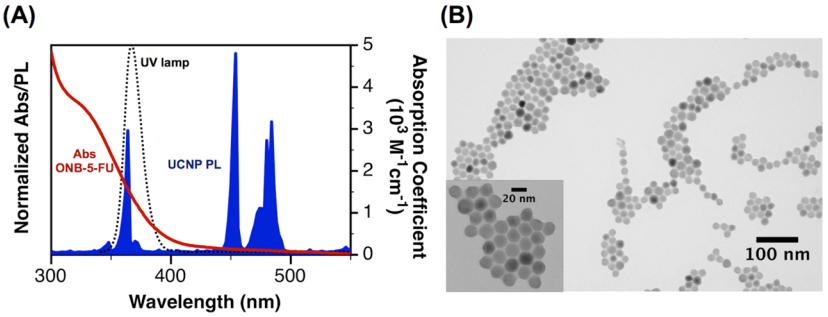

Figure 2. (A) Normalized PL spectrum of $NaYF_4$ (4.95% Yb, 0.08% Tm) core−shell UCNPs upon irradiation with a 980 nm laser (blue line) and UV−vis absorption spectra of the ONB−FU prodrug (red line). The molar absorption coefficient of the ONB−FU prodrug is 1560 M^{-1} cm^{-1} at 364 nm. The UCNP PL spectrum is normalized to the most intense UV−vis emission at 454 nm. The normalized emission profile of the UV lamp with a maximum at 367 nm used for direct UV photocleavage is shown as a black dashed line. (B) TEM image of oleic acid-capped UCNPs.

maintained for 1 h. The product was collected by centrifugation (4500 rpm for 8 min), washed with anhydrous ethanol several times, and dispersed in hexane. The presence of UC was visually confirmed by blue emission upon NIR (980 nm) irradiation.

In a subsequent shell growth procedure, 0.4586 g of $Y(CH_3CO_2)_3$ was combined in a 150 mL three-neck round-bottom flask with 30 mL of 1-octadecene and 12 mL of oleic acid, and the reaction mixture was heated to 115 °C while being stirred for 30 min under vacuum. The temperature was then decreased to 80 °C under an argon atmosphere, and the core UCNPs dispersed in hexane were added. After hexane was removed, the temperature was decreased to 50 °C, and 20 mL of a methanol solution with 0.2966 g of NH_4F and 0.1904 g of NaOH was added to the reaction mixture and the mixture stirred for an additional 30 min. The cloudy solution was heated to 70 °C to remove excess methanol. The temperature was then increased to 300 °C for 1 h. The product was collected by centrifugation (4500 rpm for 8 min), washed several times with anhydrous ethanol, and dispersed in hexane. The UC nanocrystals exhibited blue emission upon NIR (980 nm) irradiation. The UCNPs were characterized using inductively coupled plasma−atomic emission spectroscopy (ICP−AES), luminescence spectroscopy, and transmission electron microscopy (TEM).

Ligand Exchange of β-$NaYF_4$: Yb, Tm UCNPs. A total of 100 mg of oleic acid-capped UCNPs in ∼1 mL of hexane was mixed with 400 mg (2.84 mmol) of *o*-phosphorylethanolamine in 1 mL of 25% (w/v) tetramethylammonium hydroxide in methanol and 4 mL of anhydrous ethanol. This mixture was vortexed and allowed to stir at 70 °C overnight. The nanoparticles were then precipitated with hexane and washed three times by centrifugation at 4500 rpm for 8 min with deionized (DI) water. The presence of primary amines on the UCNPs was confirmed using ninhydrin reagent.

Preparation of UCNP Conjugates with a Photocleavable ONB−5-FU Prodrug. The ONB−5-FU prodrug was synthesized via a six-step process, and all of the steps were characterized using nuclear magnetic resonance (NMR) and mass spectrometry (MS) (see the Supporting Information for details).

A 2.0 mg (4.8 μmol) quantity of the ONB−5-FU prodrug was combined with 80 mg (0.7 mmol) of *N*-hydroxysuccinimide in 0.5 mL of dimethyl sulfoxide (DMSO). The mixture was purged with nitrogen and stirred until it became clear. A 0.50 mL (0.74 nmol) volume of a 14.7 mg mL^{-1} solution of *o*-phosphorylethanolamine-capped UCNPs dispersed in DMSO was then added, and the mixture was stirred for 5 min. A 0.08 mL (0.5 mmol) volume of *N*,*N*′-diisopropylcarbodiimide was diluted to 0.16 mL with DMSO and added dropwise to the mixture while it was being vigorously stirred. The mixture was stirred for 24 h at room temperature under nitrogen. The nanoparticles were then separated and washed with a 1:1 (v/v) methanol/DI water mixture by centrifugation at 11000 rpm for 30 min, and the wash process was repeated four more times. The supernatant was placed on the C-18 RP-HPLC column, using a 1:1 (v/v) methanol/DI water mixture as the mobile phase to ensure that free 5-FU, ONB−FU prodrug, and residual *o*-phosphorylamine ligands were not present. The UCNP−ONB−FU conjugates were redissolved in DI water and stored at 4 °C. The conjugation was confirmed by UV−vis absorption spectroscopy (see Figure S3 of the Supporting Information).

Light-Triggered 5-FU Drug Release Assays. The uncaging of 5-FU from the UCNP−ONB−FU conjugate was characterized by exciting 200 μL of a 2.8 mg mL^{-1} UCNP−ONB−FU solution with 365 nm (0.5 mW, power density of 0.18 mW cm^{-2}) UV irradiation and separately with 980 nm (10, 30, and 80 mW and corresponding power densities of 7.9, 23.7, and 63.2 mW cm^{-2}, respectively) NIR irradiation for various amounts of time (0−80 min). After irradiation, the solvent was removed under vacuum. The product was then redissolved in 200 μL of a 1:1 (v/v) methanol/DI water mixture and vortexed for 2 min. The nanoparticles were then separated by centrifugation at 11000 rpm for 30 min. The supernatant was collected, and standard additions of 0.05, 0.10, and 0.15 mg mL^{-1} 5-FU were made. A volume of 10 μL of the solution was injected into the HPLC column and eluted at 25 °C. The mobile phase was a 1:1 (v/v) methanol/DI water mixture, and the flow rate was 1.0 mL min^{-1}. Absorption at 256 nm was monitored. The rates of 5-FU photocleavage were computed as initial rates by differentiating the reaction biexponential progress curves with respect to time (details can be found in the eqs S1−S3 of the Supporting Information). The initial rates for the samples irradiated via both UV and NIR excitation have been calculated at 5 min.

RESULTS AND DISCUSSION

Characterization of β-$NaYF_4$: Yb, Tm−β-$NaYF_4$ Core−Shell UCNPs. The core−shell oleic acid-capped UCNPs were prepared using a two-step protocol. First, β-$NaYF_4$: 4.95% Yb, 0.08% Tm-doped core UCNPs were synthesized as described previously.[13] $NaYF_4$ was selected as the host matrix because of its close lattice match to entrain the dopant ions and characteristic low phonon energies. Tm^{3+} served as the activator ion, while Yb^{3+} acted as the sensitizer. Tm^{3+} was selected as a dopant as it offers blue-shifted emission with strong potential for PL bands residing in the UV region. Yb^{3+} was selected because it has only two multiplets, and the energy gap between the ground state and excited state offers efficient absorption in the range of 900−1000 nm. This particular energy level structure is well-suited for excitation using conventional 980 nm laser diodes. Also, Yb^{3+} has efficient emission from 1000 to 1100 nm, which offers excellent energy overlap to excite Tm^{3+}. The resulting PL emission bands range from 348 to 490 nm.[26,27] For UCNP cores consisting of these dopants, upconversion efficiencies of 0.005−0.3% have been reported for the aforementioned PL emissions.[28]

A shell layer of $NaYF_4$ served to improve the brightness of the core UCNPs by minimizing the effect of quenching due to interactions of dopant ions with solvent.[8,13,29−32] The synthesized core−shell UCNPs were characterized using a

combination of fluorescence spectroscopy, ICP–AES, and electron microscopy. The PL spectrum shown in Figure 2A displays few major emission peaks across the UV–vis region with maximal intensities at 364, 454, and 484 nm.

The average size and homogeneity of the UCNPs were determined via electron microscopy. A TEM image of the oleic acid-capped UCNPs is shown in Figure 2B. The UCNPs adopted a hexagonal structure characteristic of β-UCNP that was expected *a priori* because of the synthesis method and the temperature of the reaction.[28,33−35] The average diameter of the UCNPs was determined to be 20.1 ± 3.0 nm by physical measurement of 100 particles and indicated excellent monodispersity. The ICP–AES analysis of the nanoparticles revealed a composition of 16.34% Na, 0.076% Tm, 13.25% Y, 4.96% Yb, and 65.37% F. Assuming a spherical particle, the density of $NaYF_4$ (4.2 g cm^{-3}), and the average diameter from the electron microscopy data, the molecular weight of the nanoparticles was calculated to be 1×10^7.[36]

Conjugation of the ONB–5-FU Prodrug to UCNPs. To impart water solubility, the hydrophobic oleic acid coating was displaced with *o*-phosphorylethanolamine via ligand exchange.[28,37] The exchange was facilitated by the binding affinity of the phosphate functional group for the inorganic shell being higher than that of the carboxylate groups.[38] At physiological pH, the basic amine terminus is positively charged and provided colloidal stability to the UCNPs. Furthermore, the primary amine group facilitated coupling with the ONB–FU prodrug through amide bond formation using carbodiimide activation of the free carboxylic acid of the ONB. In addition, the compactness of the *o*-phosphorylethanolamine ligand relative to other coatings (cf. polyethylene glycol or silica encapsulation) positions the caged prodrug in the proximity of the surface of the UCNP (<2 nm). A minimal separation between a photoactive group and the emitter is beneficial for strongly distance-dependent resonance energy transfer for photocleavage assays.[39,40] The UCNP–ONB–FU conjugate was prepared by first activating the carboxylic acid on ONB using *N,N′*-diisopropylcarbodiimide and then mixing with the UCNPs to afford a stable amide linkage to the UCNP surface. Successful coupling of the ONB–FU prodrug to the UCNPs was confirmed using UV–vis absorption, as shown in Figure S3 of the Supporting Information.

The UCNPs served as platforms for caging the therapeutic agent, where the intrinsic upconversion of incident NIR radiation to UV–vis PL served as the internal trigger to release the 5-FU. The therapeutic agent, 5-FU, falls into the antimetabolite drug classification and interferes with the ability of cells to express DNA and RNA.[41] The intention of this experimental work was to demonstrate the effectiveness of the ONB linkage in NIR radiation-triggered photolysis from UCNPs using 5-FU as a model. The qualitative spectral overlap of the absoprtion by the ONB–FU prodrug and the PL emission of the UCNPs is shown in Figure 2A. The sole UV PL emission band centered at 365 nm of the UCNPs resides in an area of resonant absorption by the ONB–FU prodrug and offers potential for photocleavage of the 5-FU.

Characterization of UV Light-Triggered Photocleavage of the ONB–5-FU Prodrug. Initial characterization of photocleavage and release of 5-FU from the ONB–FU prodrug was conducted using a UV lamp (0.5 mW, 365 nm) for the samples in DI water (see the Supporting Information for details). A control sample of the ONB–FU prodrug was irradiated with 980 nm laser radiation (30 mW) to determine whether the cleavage was in fact due to UV PL (see Figure S4 of the Supporting Information). The products released in the solution were monitored using C18 RP-HPLC [1:1 (v/v) methanol/DI water mixture as the mobile phase]. The resultant chromatograms indicated a single band at a retention time of 2.76 min for the samples irradiated by the UV lamp, while no new components were detected from the samples irradiated with a 980 nm NIR laser. The identity of the released compound in the UV-irradiated samples was confirmed to be 5-FU using mass spectrometry. The proposed mechanism of the release is based on a highly reactive radical intermediate and ultimate cleavage of the C–N bond between ONB and 5-FU,[42] and details can be found elsewhere.[43]

The ability to release the caged 5-FU drug conjugated to UCNPs by UV-triggered photolysis was examined by excitation using a UV lamp. The time-dependent release of 5-FU was monitored by RP-HPLC and is shown in Figure 3. The limit of

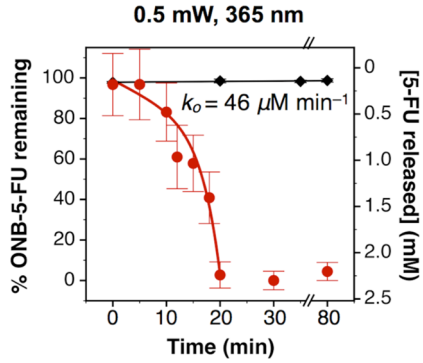

Figure 3. Progress of the release of 5-FU following irradiation of the UCNP–ONB–FU conjugates with a 0.5 mW 365 nm UV lamp (red) and a control in which conjugates were left solely in the dark (black). The biexponential curve fit is given by the solid red line where the initial rate, k_0, was 46 μM min^{-1}.

detection for the 5-FU drug molecules was 1.0×10^{-5} mg mL^{-1} (equivalent to ~1.5 released drug molecules per nanoparticle). Continuous irradiation of the samples with both UV and NIR sources could potentially cause a relative increase in temperature, which could in turn influence the release rate. When samples were irradiated with UV light (0.5 mW), a 2.2 °C temperature increase over 60 min was noted, while NIR irradiation (30 mW) resulted in an increase of 1.8 °C (see Figure S4 of the Supporting Information). Both of the excitation sources resulted in marginal temperature increases that likely did not influence the release rate over the time period required for complete cleavage. This is exemplified by Figure 3, where after UV irradiation for 20 min no additional increase in the level of release of 5-FU was detected. The extent of hydrolysis of free 5-FU in the dark over the duration of the experiments was <2%. The kinetics of release were found to be consistent with previous reports of ONB photocleavage that typically follow first- or second-order decay kinetics with a strong pH dependence, with kinetic traces obeying mono- or biexponential growth.[44−47]

The time-based release using UV irradiation provided a basis for comparison of the efficacy of the proposed NIR radiation-triggered UCNP release described in the following section. For the purpose of quantitative comparison of release rates, the progress curves were fit with a biexponential function, and an initial rate (k_0) was calculated at 5 min from fit parameters (see

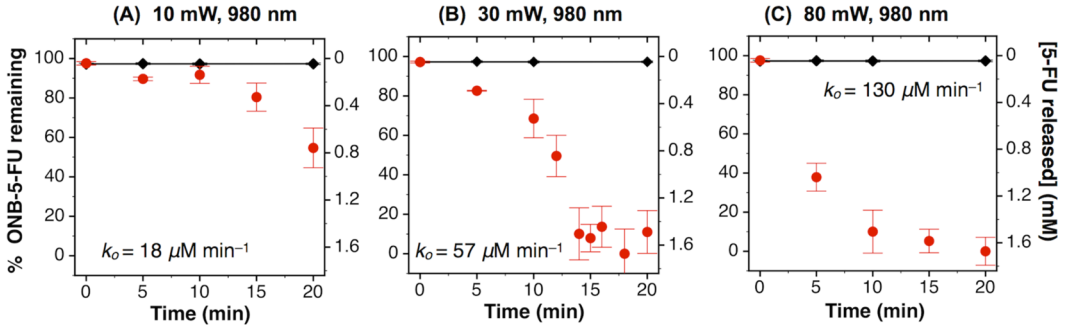

Figure 4. Progress of the release of 5-FU following irradiation of UCNP−ONB−FU samples with a 980 nm laser for various periods of time. The laser power outputs were 10 (A), 30 (B), and 80 mW (C). The corresponding initial rates increased from 18 to 57 μM min^{-1} and from 57 to 130 μM min^{-1} when the power increased from 10 to 30 mW and from 30 to 80 mW, respectively. The biexponential fit curves are shown in Figure S6 of the Supporting Information.

the Supporting Information for details). It is important to highlight that the initial rates are not representative of the photolysis mechanism using UCNP and were used solely for comparison of different irradiation conditions on the release of 5-FU.

Characterization of NIR Radiation-Mediated Release of 5-FU from UCNPs. The UCNP−ONB−FU samples prepared in DI water were irradiated with a 980 nm laser for various amounts of time. Within ∼14 min of continuous irradiation by NIR light at 30 mW, complete interfacial release of 5-FU had occurred as shown by Figure 4. The kinetic curve was fit with a biexponential equation, and the initial rate was determined to be 57 μM min^{-1} (see the Supporting Information for details). It was also observed that the rate of 5-FU release could be controlled by varying the incident NIR light intensity where 80 and 10 mW NIR laser powers resulted in different release kinetics. As shown in Figure 4, a complete photolysis was observed after ∼10 min using a power of 80 mW, where an increase in the initial rate constant was ∼2.3-fold (130 μM min^{-1}), consistent with the magnitude of the increase in the excitation power. In contrast, a decrease in the power of the NIR source to 10 mW resulted in a decrease in the initial rate to 18 μM min^{-1} (see Figure S6 of the Supporting Information).

The average maximal concentration of 5-FU molecules released from UCNPs by direct UV excitation was estimated to be 2.2 mM (Figure 3). The average maximal concentration of 5-FU molecules released under NIR irradiation was found to be 1.7 mM, indicating that the efficiency of release from the UCNPs by NIR excitation was ∼77% of that achieved by direct UV excitation. Extrapolating these *in vitro* results for potential practical application, we found nontargeted tissue structures are unaffected by NIR treatment provided the temperature remains below 42 °C. Laser powers in the range of 2−15 W with wavelengths similar to that used herein are found in clinical photothermal therapy methods.[48] Therefore, the NIR power that has been used to penetrate tissues appears to be sufficient to excite UCNPs for drug release.

CONCLUSIONS

We have shown that a common caged anticancer drug can be conjugated to upconverting nanoparticles to prepare the photosensitive release system. Via the attachment of the therapeutic via an ONB photoactivatable linker, the UCNP served as a photocaging nanocarrier. Following NIR irradiation with upconversion in the UV range, free 5-FU therapeutic was released and quantified. Excitation of decorated UCNPs with NIR radiation achieved up to 77% release of the drug in 10−15 min in comparison to direct UV illumination to trigger photolysis. Controlled rates of drug release could be achieved by selection of NIR excitation power. Importantly, the range of NIR power that was necessary for UCNP-mediated photolysis is substantially lower in comparison to laser powers commonly used in medical and clinical settings. We anticipate that the methods and strategies presented here can be extended to a wide range of therapeutics and target molecules for photo-mediated delivery. This work is an important initial step in the development of a theranostic nanocarrier for NIR imaging and drug delivery.

ASSOCIATED CONTENT

Supporting Information

Detailed experimental methods, including materials, synthesis, and characterization of the ONB−FU prodrug; data analysis; and additional results. This material is available free of charge via the Internet at http://pubs.acs.org.

AUTHOR INFORMATION

Corresponding Author

*E-mail: ulrich.krull@utoronto.ca.

Present Address

†E.P.: Department of Chemistry, University of British Columbia, 2036 Main Mall, Vancouver, British Columbia V6T 1Z1, Canada.

Notes

The authors declare no competing financial interest.

ACKNOWLEDGMENTS

We thank Dr. Feng Zhou from the Chemical Sensors Group for provision and characterization of some of the UCNPs and Dr. Sreekumari Nair for assistance with the electron microscopy work. Dr. Peter Mitrakos is also thanked for assistance with ICP−AES analysis. We acknowledge the financial support of our research program by the Natural Sciences and Engineering Research Council of Canada (NSERC). A.J.T., E.P., and S.D. are also grateful to the NSERC for postgraduate scholarships.

REFERENCES

(1) Singh, R.; Lillard, J. W., Jr. Nanoparticle-based Targeted Drug Delivery. *Exp. Mol. Pathol.* **2009**, *86*, 215−223.

(2) Wang, A. Z.; Langer, R.; Farokhzad, O. C. Nanoparticle Delivery of Cancer Drugs. *Annu. Rev. Med.* **2012**, *63*, 185−198.

(3) Parveen, S.; Misra, R.; Sahoo, S. K. Nanoparticles: A Boon to Drug Delivery, Therapeutics, Diagnostics and Imaging. *Nanomedicine* **2012**, *8*, 147−166.
(4) Zhang, L.; Li, Y. C.; Yu, J. C. Chemical Modification of Inorganic Nanostructures for Targeted and Controlled Drug Delivery in Cancer Treatment. *J. Mater. Chem. B* **2014**, *2*, 452−470.
(5) Dougherty, T. J.; Gomer, C. J.; Henderson, B. W.; Jori, G.; Kessel, D.; Korbelik, M.; Moan, J.; Peng, Q. Photodynamic Therapy. *J. Natl. Cancer Inst.* **1998**, *90*, 889−905.
(6) Brigger, I.; Dubernet, C.; Couvreur, P. Nanoparticles in Cancer Therapy and Diagnosis. *Adv. Drug Delivery Rev.* **2002**, *54*, 631−651.
(7) Anderson, R. R.; Parrish, J. A. The Optics of Human Skin. *J. Invest. Dermatol.* **1981**, *77*, 13−19.
(8) Haase, M.; Schäfer, H. Upconverting Nanoparticles. *Angew. Chem., Int. Ed.* **2011**, *50*, 5808−5829.
(9) Wang, C.; Cheng, L. A.; Liu, Z. A. Drug Delivery with Upconversion Nanoparticles for Multi-functional Targeted Cancer Cell Imaging and Therapy. *Biomaterials* **2011**, *32*, 1110−1120.
(10) Chen, C.; Yee, L. K.; Gong, H.; Zhang, Y.; Xu, R. A Facile Synthesis of Strong Near Infrared Fluorescent Layered Double Hydroxide Nanovehicles with an Anticancer Drug for Tumor Optical Imaging and Therapy. *Nanoscale* **2013**, *5*, 4314−4320.
(11) Tian, G.; Gu, Z.; Zhou, L.; Yin, W.; Liu, X.; Yan, L.; Jin, S.; Ren, W.; Xing, G.; Li, S.; Zhao, Y. Mn^{2+} Dopant-Controlled Synthesis of NaYF4:Yb/Er Upconversion Nanoparticles for in Vivo Imaging and Drug Delivery. *Adv. Mater.* **2012**, *24*, 1226−1231.
(12) Zhao, L.; Peng, J.; Huang, Q.; Li, C.; Chen, M.; Sun, Y.; Lin, Q.; Zhu, L.; Li, F. Near-Infrared Photoregulated Drug Release in Living Tumor Tissue via Yolk-Shell Upconversion Nanocages. *Adv. Funct. Mater.* **2014**, *24*, 363−371.
(13) Carling, C. J.; Nourmohammadian, F.; Boyer, J. C.; Branda, N. R. Remote-Control Photorelease of Caged Compounds Using Near-Infrared Light and Upconverting Nanoparticles. *Angew. Chem., Int. Ed.* **2010**, *49*, 3782−3785.
(14) Dai, Y.; Ma, P. a.; Cheng, Z.; Kang, X.; Zhang, X.; Hou, Z.; Li, C.; Yang, D.; Zhai, X.; Lin, J. Up-Conversion Cell Imaging and pH-Induced Thermally Controlled Drug Release from $NaYF_4$:Yb^{3+}/Er^{3+}@ Hydrogel Core−Shell Hybrid Microspheres. *ACS Nano* **2012**, *6*, 3327−3338.
(15) Yang, Y.; Velmurugan, B.; Liu, X.; Xing, B. NIR Photoresponsive Crosslinked Upconverting Nanocarriers Toward Selective Intracellular Drug Release. *Small* **2013**, *9*, 2937−2944.
(16) Yan, B.; Boyer, J. C.; Branda, N. R.; Zhao, Y. Near-Infrared Light-Triggered Dissociation of Block Copolymer Micelles Using Upconverting Nanoparticles. *J. Am. Chem. Soc.* **2011**, *133*, 19714−19717.
(17) Dai, Y.; Xiao, H.; Liu, J.; Yuan, Q.; Ma, P. a.; Yang, D.; Li, C.; Cheng, Z.; Hou, Z.; Yang, P.; Lin, J. In Vivo Multimodality Imaging and Cancer Therapy by Near-Infrared Light-Triggered trans-Platinum Pro-Drug-Conjugated Upconverison Nanoparticles. *J. Am. Chem. Soc.* **2013**, *135*, 18920−18929.
(18) Zhou, A.; Wei, Y.; Wu, B.; Chen, Q.; Xing, D. Pyropheophorbide A and c(RGDyK) Comodified Chitosan-Wrapped Upconversion Nanoparticle for Targeted Near-Infrared Photodynamic Therapy. *Mol. Pharmaceutics* **2012**, *9*, 1580−1589.
(19) Cui, S.; Yin, D.; Chen, Y.; Di, Y.; Chen, H.; Ma, Y.; Achilefu, S.; Gu, Y. In Vivo Targeted Deep-Tissue Photodynamic Therapy Based on Near-Infrared Light Triggered Upconversion Nanoconstruct. *ACS Nano* **2013**, *7*, 676−688.
(20) Liu, K.; Liu, X.; Zeng, Q.; Zhang, Y.; Tu, L.; Liu, T.; Kong, X.; Wang, Y.; Cao, F.; Lambrechts, S. A. G.; Aalders, M. C. G.; Zhang, H. Covalently Assembled NIR Nanoplatform for Simultaneous Fluorescence Imaging and Photodynamic Therapy of Cancer Cells. *ACS Nano* **2012**, *6*, 4054−4062.
(21) Zhou, L.; Chen, Z.; Dong, K.; Yin, M.; Ren, J.; Qu, X. DNA-mediated Construction of Hollow Upconversion Nanoparticles for Protein Harvesting and Near-Infrared Light Triggered Release. *Adv. Mater.* **2014**, *26*, 2424−2430.
(22) Viger, M. L.; Grossman, M.; Fomina, N.; Almutairi, A. Low Power Upconverted Near-IR Light for Efficient Polymeric Nanoparticle Degradation and Cargo Release. *Adv. Mater.* **2013**, *25*, 3733−3738.
(23) Chien, Y. H.; Chou, Y. L.; Wang, S. W.; Hung, S. T.; Liau, M. C.; Chao, Y. J.; Su, C. H.; Yeh, C. S. Near-Infrared Light Photocontrolled Targeting, Bioimaging, and Chemotherapy with Caged Upconversion Nanoparticles in Vitro and in Vivo. *ACS Nano* **2013**, *7*, 8516−8528.
(24) Agasti, S. S.; Chompoosor, A.; You, C. C.; Ghosh, P.; Kim, C. K.; Rotello, V. M. Photoregulated Release of Caged Anticancer Drugs from Gold Nanoparticles. *J. Am. Chem. Soc.* **2009**, *131*, 5728−5729.
(25) Patchornik, A.; Amit, B.; Woodward, R. B. Photosensitive Protecting Groups. *J. Am. Chem. Soc.* **1970**, *92*, 6333−6335.
(26) Carnall, W. T.; Goodman, G. L.; Rajnak, K.; Rana, R. S. A Systematic Analysis of the Spectra of the Lanthanides Doped into Single Crystal LaF_3. *J. Chem. Phys.* **1989**, *90*, 3443−3457.
(27) Eliseeva, S. V.; Bünzli, J. G. Lanthanide Luminescence for Functional Materials and Bio-Sciences. *Chem. Soc. Rev.* **2010**, *39*, 189−227.
(28) Boyer, J.-C.; van Veggel, F. C. J. M. Absolute Quantum Yield Measurements of Colloidal NaYF4: Er^{3+}, Yb^{3+} Upconverting Nanoparticles. *Nanoscale* **2010**, *2*, 1417−1419.
(29) Yi, G.-S.; Chow, G.-M. Water-Soluble $NaYF_4$:Yb,Er(Tm)/$NaYF_4$/Polymer Core/Shell/Shell Nanoparticles with Significant Enhancement of Upconversion Fluorescence. *Chem. Mater.* **2007**, *19*, 341−343.
(30) Mai, H.-X.; Zhang, Y.-W.; Sun, L.-D.; Yan, C.-H. Highly Efficient Multicolor Up-Conversion Emissions and Their Mechanisms of Monodisperse $NaYF_4$:YB,Er Core and Core/Shell-Structured Nanocrystals. *J. Phys. Chem. C* **2007**, *111*, 13721−13729.
(31) Ghosh, P.; Oliva, J.; De la Rosa, E.; Kanta Haldar, K.; Solis, D.; Patra, A. Enhancement of Upconversion Emission of $LaPO_4$:Er@Yb Core-Shell Nanoparticles/Nanorods. *J. Phys. Chem. C* **2008**, *112*, 9650−9658.
(32) Feng, W.; Han, C.; Li, F. Upconversion-Nanophosphor-Based Functional Nanocomposites. *Adv. Mater.* **2013**, *25*, 5287−5829.
(33) Boyer, J. C.; Cuccia, L. A.; Capobianco, J. A. Synthesis of Colloidal Upconverting $NaYF_4$: Er^{3+}/Yb^{3+} and Tm^{3+}/Yb^{3+} Monodisperse Nanocrystals. *Nano Lett.* **2007**, *7*, 847−852.
(34) He, M.; Huang, P.; Zhang, C.; Hu, H.; Bao, C.; Gao, G.; He, R.; Cui, D. Dual Phase-Controlled Synthesis of Uniform Lanthanide-Doped $NaGdF_4$ Upconversion Nanocrystals Via an OA/Ionic Liquid Two-Phase System for In Vivo Dual-Modality Imaging. *Adv. Funct. Mater.* **2011**, *21*, 4470−4477.
(35) Huang, W.; Ding, M.; Huang, H.; Jiang, C.; Song, Y.; Ni, Y.; Lu, C.; Xu, Z. Uniform $NaYF_4$:Yb, Tm Hexagonal Submicroplates: Controlled Synthesis and Enhanced UV and Blue Upconversion Luminescence. *Mater. Res. Bull.* **2013**, *48*, 300−304.
(36) Cheng, L.; Yang, K.; Zhang, S.; Shao, M.; Lee, S.; Liu, Z. Highly-Sensitive Multiplexed In Vivo Imaging Using PEGylated Upconversion Nanoparticles. *Nano Res.* **2010**, *3*, 722−732.
(37) Xiong, L. Q.; Chen, Z. G.; Yu, M. X.; Li, F. Y.; Liu, C.; Huang, C. H. Synthesis, Characterization, and In Vivo Targeted Imaging of Amine-functionalized Rare-Earth Up-Converting Nanophosphors. *Biomaterials* **2009**, *30*, 5592−5600.
(38) Remko, M.; Van Duijnen, P. T.; von der Lieth, C. W. Structure and Stability of Li(I) and Na(I)−Carboxylate, Sulfate and Phosphate Complexes. *THEOCHEM* **2007**, *814*, 119−125.
(39) Zhou, F.; Noor, M. O.; Krull, U. J. Luminescence Resonance Energy Transfer-Based Nucleic Acid Hybridization Assay on Cellulose Paper with Upconverting Phosphor as Donors. *Anal. Chem.* **2014**, *86*, 2719−2726.
(40) DaCosta, M. V.; Doughan, S.; Han, Y.; Krull, U. J. Lanthanide Upconversion Nanoparticles and Applications in Bioassays and Bioimaging: A Review. *Anal. Chim. Acta* **2014**, *832*, 1−33.
(41) Bunz, F.; Hwang, P. M.; Torrance, C.; Waldman, T.; Zhang, Y.; Dillehay, L.; Williams, J.; Lengauer, C.; Kinzler, K. W.; Vogelstein, B.

Disruption of P53 in Human Cancer Cells Alters the Responses to Therapeutic Agents. *J. Clin. Invest.* **1999**, *104*, 263−269.
(42) Yu, H.; Li, J.; Wu, D.; Qiu, Z.; Zhang, Y. Chemistry and Biological Applications of Photo-labile Organic Molecules. *Chem. Soc. Rev.* **2010**, *39*, 464−473.
(43) Pelliccioli, A. P.; Wirz, J. Photoremovable Protecting Groups: Reaction Mechanisms and Applications. *Photochem. Photobiol. Sci.* **2002**, *1*, 441−458.
(44) Hu, J.; Zhang, J.; Liu, F.; Kittredge, K.; Whitesell, J. K.; Fox, M. A. Competitive Photochemical Reactivity in a Self-Assembled Monolayer on a Colloidal Gold Cluster. *J. Am. Chem. Soc.* **2001**, *123*, 1464−1470.
(45) Mathew, T.; Ajayaghosh, A.; Das, S.; Kamat, P. V.; George, M. V. A New Photodegradable Polyamide Containing o-nitrobenzyl Chromophore. Steady State and Laser Flash Photolysis Studies. *J. Photochem. Photobiol., A* **1993**, *71*, 181−189.
(46) Piggott, A. M.; Karuso, P. Synthesis of a New Hydrophilic o-nitrobenzyl Photocleavable Linker Suitable for use in Chemical Proteomics. *Tetrahedron Lett.* **2005**, *46*, 8241−8244.
(47) Il'ichev, Y. V.; Schwörer, M. A.; Wirz, J. Photochemical Reaction Mechanisms of 2-Nitrobenzyl Compounds: Methyl Ethers and Caged ATP. *J. Am. Chem. Soc.* **2004**, *126*, 4581−4595.
(48) Colin, P.; Mordon, S.; Nevoux, P.; Marqa, M. F.; Ouzzane, A.; Puech, P.; Bozzini, G.; Leroux, B.; Villers, A.; Betrouni, N. Focal Laser Ablation of Prostate Cancer: Definition, Needs, and Future. *Adv. Urol.* **2012**, *2012*, 10.